Technical Note

Effect of infilled materials and arrangements on shear characteristics of stacked soilbags

K. Fan[1], S. H. Liu[2], Y. P. (Helen) Cheng[3] and J. Liao[4]

[1]PhD candidate, College of Water Conservancy and Hydropower, Hohai University, Nanjing 210098, China; Visiting researcher, Civil, Environmental and Geomatic Engineering, University College London, London WC1E 6BT, UK, E-mail: kw_fan@hhu.edu.cn
[2]Professor, College of Water Conservancy and Hydropower, Hohai University, Nanjing 210098, China, E-mail: sihongliu@hhu.edu.cn (corresponding author)
[3]Associate Professor, Civil, Environmental and Geomatic Engineering, University College London, London WC1E 6BT, UK, E-mail: yi.cheng@ucl.ac.uk
[4]PhD candidate, College of Water Conservancy and Hydropower, Hohai University, Nanjing 210098, China, E-mail: liaojiehhu@gmail.com

Received 01 October 2019, revised 16 December 2019, accepted 19 April 2020

ABSTRACT: The shear characteristics of stacked soilbags are related to their interlayer arrangements and the properties of the materials with which the bags (geosynthetics) are filled. To study the effects of those factors on the shear strength and failure mode of stacked soilbags, a series of shear tests were conducted. The results show that although the shear failure surface occurred at the horizontal interface between soilbags when they were stacked vertically, it was ladder-like when the soilbags were stacked in a staggered manner. The angle of insertion was found to govern the shape of the shear failure surface and, thus, the final shear strength of soilbags stacked in a staggered manner. Two shear failure modes of the stacked soilbags were observed with different infilled materials. When the frictional resistance of the contact interface was smaller than the shear strength of the materials with which the bags was filled, only interlayer sliding failure occurred. Otherwise, the simple shear failure of materials filling the bags occurred first, followed by interlayer sliding failure.

KEYWORDS: Geosynthetics, Soilbag, Contact interface, Shear failure model, Shear strength

REFERENCE: Fan, K., Liu, S. H., Cheng, Y. P. (Helen) and Liao, J. (2020). Effect of infilled materials and arrangements on shear characteristics of stacked soilbags. *Geosynthetics International*. [https://doi.org/10.1680/jgein.20.00019]

1. INTRODUCTION

Soilbags or, more precisely, geotextile bags filled with soils or soil-like materials, have high compressive strength (Liu *et al*. 2012; Li *et al*. 2013; Cheng *et al*. 2016). For example, an ordinary polypropylene bag filled with crushed stones or sand (approximately $40 \times 40 \times 10$ cm) can withstand a load of up to 230–280 kN. Therefore, soilbags are also known as 'soft stone'. Matsuoka and Liu (2003) found that the high compressive strength of soilbags can be theoretically explained by the increased apparent cohesion that develops due to the tensile force of the wrapped bag under external loading. They modified soilbags to reinforce building foundations. Soilbags have now been used to reinforce hundreds of foundations in Japan and China (Xu *et al*. 2008; Liu *et al*. 2014; Matsuoka and Liu 2014; Ding *et al*. 2017; Liu 2017). They have many advantages such as low cost, environmental friendliness, reduced traffic-induced vibration, and the ability to prevent frost heave.

The use of soilbags has recently extended to earth-retaining structures, such as retaining walls (Portelinha *et al*. 2014; Wang *et al*. 2015; Liu *et al*. 2019) and slopes (Liu *et al*. 2012, 2015; Wang *et al*. 2019). Many researchers have claimed that the stability of earth-retaining structures constructed using soilbags is closely related to their interlayer friction, on which considerable research has been conducted using shear tests (Lohani *et al*. 2006; Krahn *et al*. 2007; Matsushima *et al*. 2008; Basudhar 2010; Ansari *et al*. 2011; Liu *et al*. 2016). The relevant studies produced a vast amount of data on the interlayer friction in engineering structures built using

soilbags. However, the only interlayer sliding failure mode with shear plane is considered when stacked soilbags are subjected to shear forces, and interlayer frictional resistance between vertically stacked soilbags is treated as their shear strength. However, Fan *et al.* (2019) found that the sliding surface in a model retaining wall stacked in a staggered manner is ladder-like due to the insertion of soilbags. The soilbag is a composite of woven bags and the materials filling them. The shear strength and deformation of soilbags may be related not only to the interlayer friction of woven bags, but also to the mechanical properties of the materials with which they are filled, which vary between pure sand and coarse-grained soil (pebbles).

In this paper, a series of shear tests on soilbags, packed with two materials of different grain sizes and stacked up in two interlayer arrangements, were conducted to study the effect of materials filling the bags and the interlayer arrangements on the shear strength and failure mode of the stacked soilbags.

2. TESTING SCHEMES AND MATERIALS

Soilbags are usually stacked either vertically or in a staggered manner in engineering practice and are filled with soils excavated from the field. Different arrangements and grain sizes of the filling materials can lead to different contact interfaces. Figure 1a shows a flat contact interface of vertically stacked soilbags with fine-grain fill (sand), while Figure 1b shows an uneven contact interface of vertically arranged soilbags with coarse-grain fill (pebbles). The effect of the uneven contact interface is defined as 'interlock' in this paper. Figure 1c shows soilbags stacked in a staggered manner. Due to their flexibility, soilbags in the upper layer can deform into gaps between two connected soilbags in the lower layer with embedded contact when subjected to vertical load. This is defined as 'insertion' in this paper. To study the shear characteristics of stacked soilbags with materials of different grain sizes filling them and the interlayer arrangements, four shear tests were designed (Table 1). Three layers of sand-filled soilbags, or soilbags filled with pebbles, were vertically stacked to observe the deformation in the stacked soilbags more clearly.

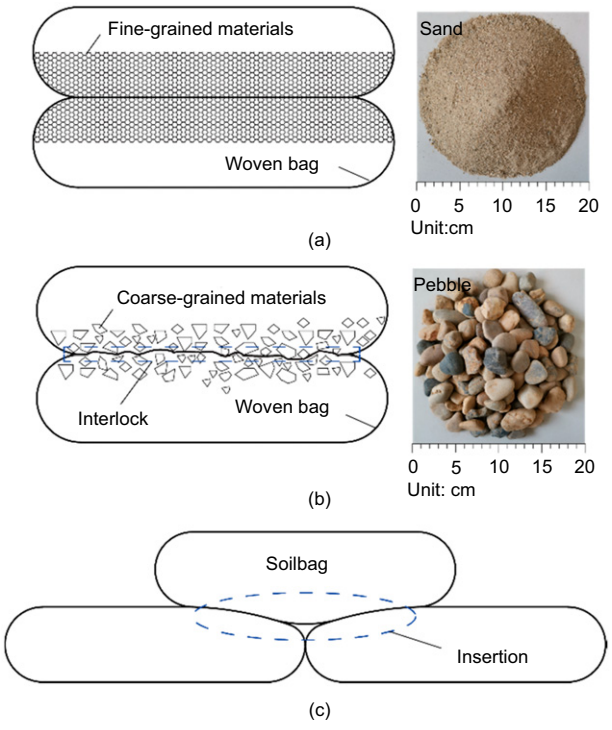

Figure 1. Schematic view of the insertion and interlock of stacked soilbags: in vertically stacked soilbags filled with (a) fine-grain materials, (b) coarse-grain material, and (c) soilbags stacked in a staggered manner

Soilbags of size $40 \times 40 \times 10$ cm, which are typically used in engineering practice (Matsuoka and Liu 2003; Xu *et al.* 2008; Liu *et al.* 2015), were used in the shear tests. The woven bags were made of polypropylene and weighed 150 g/m^2, and the coefficient of friction between two sheets of the bags was 0.34. To prevent the woven bags from being damaged by pebble particles, most of the filled pebbles were nearly elliptical in shape. Moreover, the surface of the pebbles was very smooth. The physical and mechanical properties of the infilled sand and pebbles are listed in Table 2. The initial densities of the sand and pebbles inside the woven bags were 1.63 g/cm^2 and 1.68 g/cm^2, respectively.

3. TESTING APPARATUS

A direct shear test apparatus was designed to test the shear characteristics of the stacked soilbags, as shown in Figure 2. The samples of the stacked soilbags were placed on a steel base plate so that their bottom layers could be fixed onto the base plate by two angle plates made of steel. A rigid, rough metal loading plate with two side plates was placed on top of the sample. The soilbag in the top layer was sandwiched between the side plates so that they could move with the loading plate. A displacement transducer was fixed onto the side plate to monitor horizontal displacement. The left end of the loading plate was connected to a horizontal tension device. The height of the tension device could be adjusted with the height of the sample by rotating the screw caps on the screw rods. A horizontal tension force was applied at a speed of 2 mm/min by a screw rotation axle, and a load cell was fixed to the left of the tension device to monitor the horizontal force. Vertical loads were applied to the loading plate by a motor. Some ball bearings were set between the loading plate and the vertical loading device to reduce the

Table 1. Program of shear tests on soilbags

Test	Materials	Interlayer arrangement	No. of layers
T1S	Sand	Vertically	3
T2S	Sand	Staggered	2
T1P	Pebbles	Vertically	3
T2P	Pebbles	Staggered	2

Table 2. Physical and mechanical parameters of soilbags filled with sand and pebbles

Materials	D_{30} (mm)	D_{50} (mm)	D_{60} (mm)	D_{90} (mm)	ρ_{min}	ρ_{max}	c	ϕ_{peak} (°)
Natural river sand	0.32	0.36	0.4	0.75	1.43	1.77	0	35.4
Pebbles	21.2	28.7	32.4	45.6	1.62	2.01	0	29.2

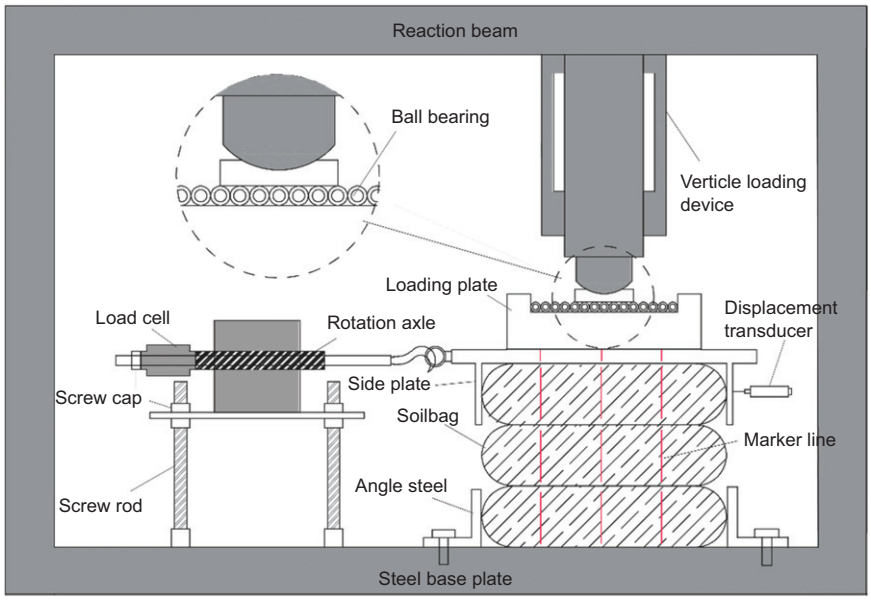

Figure 2. Schematic view of the shear test on stacked soilbags

friction between them. Several (red) marker lines, as shown in Figure 2, were placed on the soilbags and the metal loading plate to obtain the deformation and slip surface of the soilbags by measuring the relative displacement of the marker lines. The spacing between vertical lines was 10 cm. Finally, a camera was positioned in front of the setup of the shear tests to monitor the movement of the markers at regular intervals.

4. TEST RESULTS

4.1. Soilbags filled with sand

Figure 3 shows the horizontal shear stress plotted against shear displacement in tests T1S and T2S when the applied normal stress is at $\sigma_n = 80$ kPa. The development of the stress-displacement curve can be divided into two stages for T1S and three stages for T2S. The shear stress increased with the shear displacement in the first stage, OA, which was similar in both T1S and T2S. Although test T2S featured slightly higher shear stress in the first stage, the impact was minimal. In this stage, the end of the soilbag at which force was applied was first locally compressed by the shear force due to the flexibility of the soilbag filled with sand. This can be verified by the phenomenon shown in Figure 4, where the marker lines on the metal loading plate move away from those on the soilbags in the top layer. When the shear stress reached the maximum shear resistance of the contact interface between the soilbags, the soilbag in the top layer slid

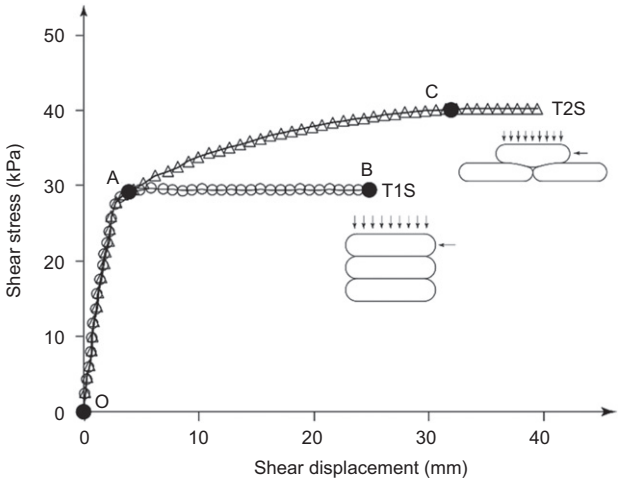

Figure 3. Shear stress versus shear displacement in tests T1S and T2S at $\sigma_n = 80$ kPa

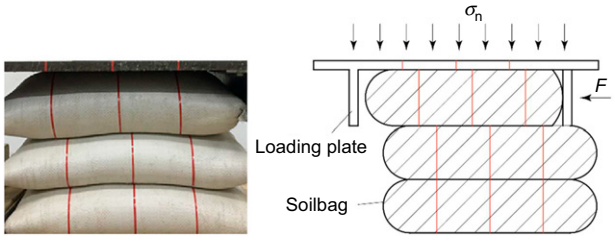

Figure 4. Deformation of soilbags during shearing in T1S

relative to the soilbag in the middle layer (see Figure 4). In stage AB of test T1S, the shear stress remained constant. For test T2S, the soilbag in the top layer deformed to settle into the gap between soilbags (insertion) in the lower layer owing to the vertical load and the flexibility of the soilbags. This insertion prevented the upper soilbag from sliding immediately at point A in T2S. During stage AC, the end of the soilbag was further compressed. However, there was an additional increase in shear stress (Stage AC) before it reached the maximum shear strength in test T2S. Also, a horizontal stress was mobilised due to the inclined angles of the soilbag interface, reducing the efficiency of the interface friction. This is verified further in Figure 7 and Equation (5) below. Finally, the shear stress reached the maximum shear strength and the soilbag in the top layer began to slide as a whole at point C.

Figure 5 presents the relationship between the final shear stress and normal stress in the tests T1S and T2S. It is clear that the final stress in T2S was greater than that in T1S under the same normal stress due to insertion. The calculated shear stress, τ_f, versus normal stress, σ_n, of the woven bags based on the friction angle, ϕ_{bag}, is also shown in Figure 5, from which it is clear that the peak shear strength of the sand-filled soilbags was only slightly larger than that of the woven bags. This is because the sand particles were sufficiently small that some were pushed out of the woven bags, and became trapped in the contact interface between soilbags. These sand particles slightly increased the sliding resistance. The curve of the peak shear strength for test T2S was always higher than that for T1S due to the mechanism explained earlier in Section 4.1 and was not straight. This was related to the measured angle of insertion shown in Figure 6. It increased as normal stress increased. To quantify the relationship between the shear force and the angle of insertion, the force acting on the upper soilbag in test T2S was analysed using the data shown in Figure 7.

If it is assumed that the contact interface between the soilbags was composed of two inclined surfaces at the same angle of inclination, θ, the height, H, and length, B, of the soilbag were assumed to be unchanged under

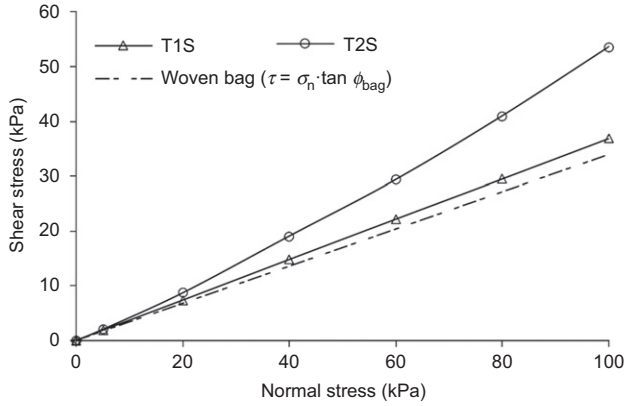

Figure 5. Final shear stress versus normal stress in T1S and T2S

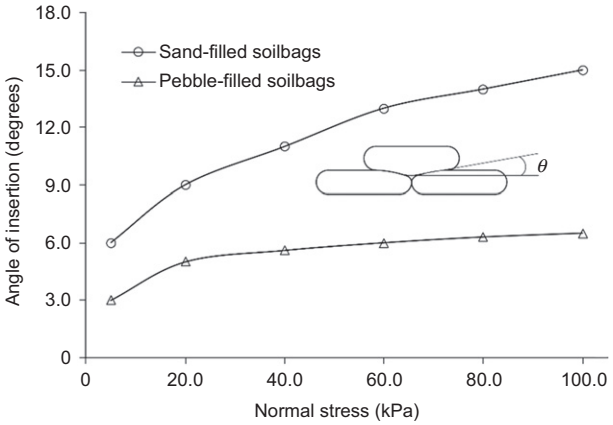

Figure 6. Angle of insertion versus normal stress in tests T2S and T2P

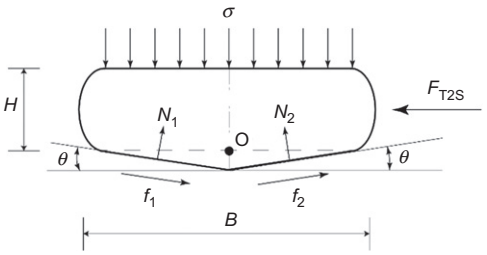

Figure 7. Analysis model for T2S

normal stress. The forces acting on the soilbag consist of the normal stress, σ (normal stress produced by dead-weight of the soilbags was calculated together with stress, σ_n), the reactions at the bottom of the soilbags N_1 and N_2, the corresponding friction, f_1 ($f_1 = \mu N_1$), and f_2 ($f_2 = \mu N_2$), and the shear force, F_{T2S}. The coefficient of interface friction of two vertically stacked soilbags filled with sand is given by μ. Using the equations of the equilibria of force and moment about point O, the following can be obtained

$$\sum F_x = 0 : (N_1 - N_2)\sin\theta + (N_1 + N_2)\mu\cos\theta = F_{T2S} \quad (1)$$

$$\sum F_y = 0 : (N_1 + N_2)\cos\theta - (N_1 - N_2)\mu\sin\theta = \sigma B \quad (2)$$

$$\sum M = 0 : (N_1 + N_2)\mu B/2 \cdot \sin\theta + (N_2 - N_1)B/4 \cdot (1 - 2\sin^2\theta)/\cos\theta + 1/2F_{T2S}H = 0 \quad (3)$$

Solving for F_{T2S}

$$F_{T2S} = \beta\mu\sigma B = \beta F_{T1S} \quad (4)$$

where

$$\beta = \frac{B}{-B + 2B(1+\mu^2)\sin^2\theta + H(1+\mu^2)\sin 2\theta} \quad (5)$$

From Equation (4) we see that the shear force with insertion, F_{T2S}, compared with the shear force without insertion F_{T1S} ($F_{T1S} = \mu\sigma B$), was scaled by β, when $\beta > 1$. β was related to the angle of insertion θ. The calculated coefficient β versus normal stress is shown in Figure 8, from which it is clear that β, as calculated from Equation (5) using the observed insertion θ, agreed reasonably well with the experimentally derived β, where $\beta = (\tau_f/\sigma_n)/\mu$, τ_f is the measured final shear stress and σ_n is the normal stress. Moreover, β reached a value of up to 1.41 under a normal stress of 100 kPa, which means that insertion can significantly increase the interlayer friction of the soilbags. This phenomenon is beneficial to the stability of a structure built using soilbags.

However, through the shear tests on five layers of soilbags stacked in a staggered manner under different vertical loads, Fan *et al.* (2019) found that the sliding surface in the shear tests was nearly horizontal under small vertical loads and ladder-like under large vertical loads, as shown in Figure 9. The shape of the sliding surface changed from being a horizontal line to a ladder-like shape because the insertion of the soilbags increased with the vertical load. Therefore, in the case of large vertical loads, the shear strength should not be calculated using Equation (4) because the sliding surface has changed. Instead, the methods proposed by Fan *et al.* (2019) should be used.

4.2. Soilbags filled with pebbles

Figure 10a shows the shear stress versus shear displacement for tests T1P (for soilbags filled with pebbles) and T1S (for soilbags filled with sand), both of which featured vertically stacked soilbags. It is clear that the shear stress-displacement curves in test T1P were not identical to those of T1S. Stage OA was nearly identical for both tests, implying that the soilbag was initially compressed by the horizontal shear force. Stage DB in test T1P featured the same mechanism as stage AB in test T1S, and the soilbag in the top layer slid relative to that in the middle layer (see Figure 11b). However, stage AD in T1P did not exist in T1S due to the deformation of the soilbag filled with pebbles before they slid, and the mechanism is shown through the shear stress-strain curved plotted in Figure 10b. The rotational shear strain, γ, increased because the shear stress caused the soilbags to deform into a parallelogram, as shown in Figure 11a. However, no rotational shear strain was observed in test T1S. This is discussed later in Section 5.

The shear stresses in the middle, stable part (AC) and the final, stable part (DB) in T1P are called the intermediate shear stress, τ_{int}, and final shear stress, τ_f, respectively. Figure 12 plots the final shear stress versus normal stress. It is clear that the final shear stress was larger than that of the woven bags, τ_{bag}, but was smaller than that of the pebbles, τ_{pebble}. This implies that the use of woven bags reduced the frictional coefficient of the pebbles, or that the use of pebbles increased the frictional coefficient of the woven bags.

The measured angle of insertion of shear tests on the soilbags filled with pebbles is plotted in Figure 6. It is clear from this that the insertion angle of soilbags filled with pebbles was smaller than that of the soilbags filled with sand. This is because the size of the pebbles was larger than that of the sand particles, which made soilbags filled with pebbles more difficult to deform and fill gaps between soilbags in the bottom layer. This will cause β calculated from Equation (5) of soilbags filled with pebbles smaller than that of soilbags filled with sand under the same vertical load, which means that the insertion of soilbags filled with pebbles is smaller than that of sand-filled soilbags. Figure 13 shows the final shear stress versus normal stress for T2S and T2P. It shows that the final stresses for tests T2S and T2P were significantly larger than those of the woven bags as a result of insertion and interlock. However, insertion played a dominant role in influencing the shear strength of stacked soilbags filled with small and regular shaped particles (sand), whereas interlocking was dominant for stacked soilbags filled with large and irregularly shaped particles (pebbles).

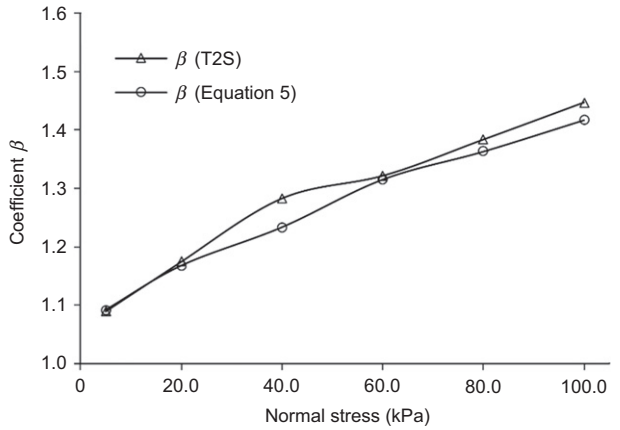

Figure 8. Coefficient β versus normal stress in T2S

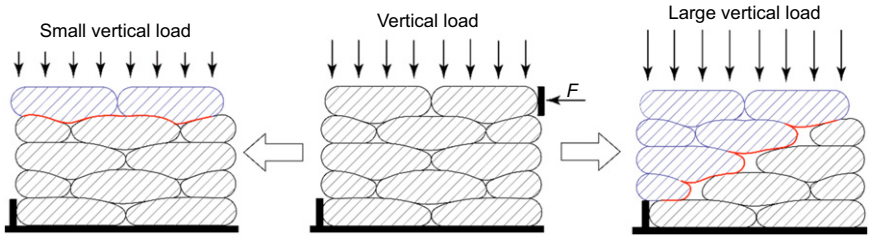

Figure 9. Different sliding surfaces in shear tests on five-layer soilbags

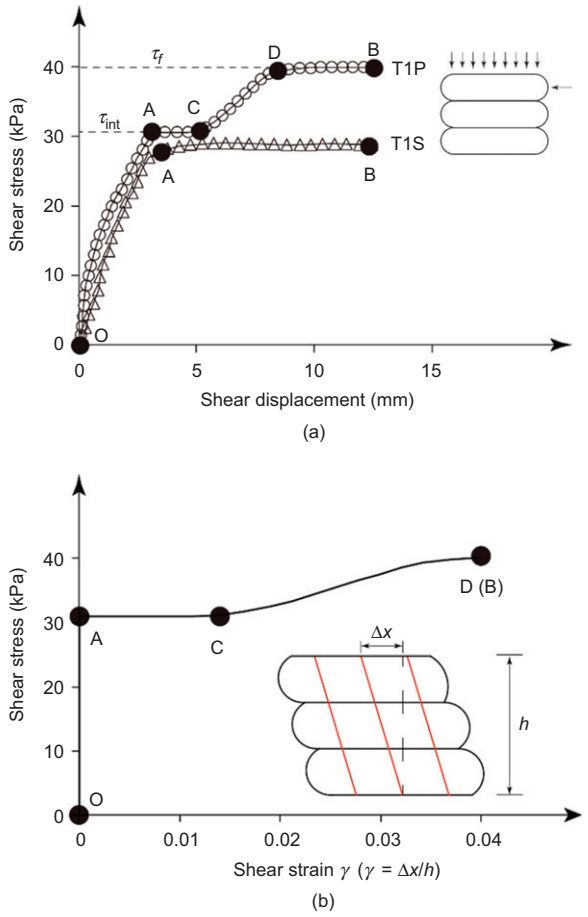

Figure 10. Shear stress versus shear displacement and shear strain (rotation) in tests T1S and T1P at $\sigma_n = 80$ kPa: (a) shear stress versus shear displacement and (b) shear stress versus shear strain

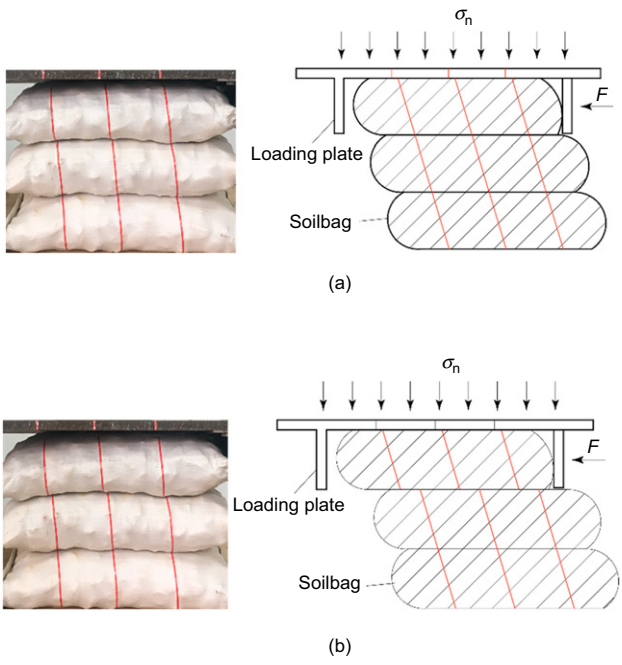

Figure 11. Status of soilbags filled with pebbles during shearing in T1P: (a) deformation of materials filling the bag in T1P and (b) interlayer sliding failure

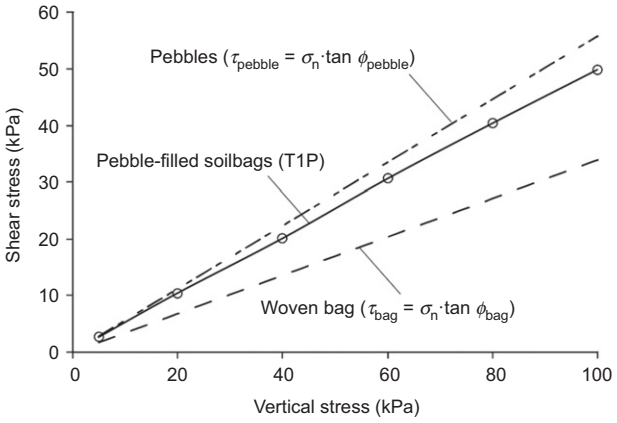

Figure 12. Final shear stress versus normal stress in test T1P

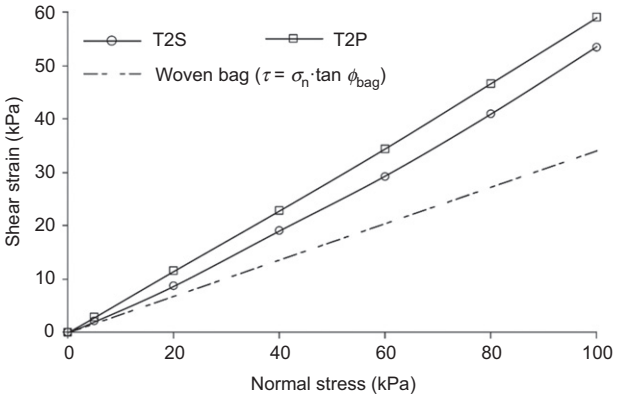

Figure 13. Final shear stress versus normal stress in test T2S and T2P

5. DISCUSSION

To determine why the soilbags filled with pebbles initially underwent shear deformation during shearing, whereas the sand-filled soilbags did not, the state of stress of an element inside the soilbags under normal stress, σ_n, was analysed. Under normal stress, the compression deformation of the soil caused the perimeter of the bag to increase, which led to and induced tensile force T along the bag (Matsuoka and Liu 2003). In practice, the induced tension may not be uniform along the bag but was assumed to be constant here throughout the bag. Figure 14a shows a 2D element of soil (either sand or pebbles) inside the soilbags in the middle layer. The forces acting on this element consisted of the normal stress $\sigma_z = \sigma_n + 2\,T/B$, lateral stress $\sigma_x = 2\,T/H$, and shear stress, τ, assuming no slip between the woven bag and the materials filling it. A Mohr circle for the element was drawn, as shown in Figure 14b. With increasing shear stress during shearing, the radius of the Mohr circle increased. When the Mohr circle touched the Coulomb failure line of the materials filling the soilbags, the materials reached failure with large deformation. The shear stress that caused them to deform is defined as the critical shear stress, τ_{crit} and can be

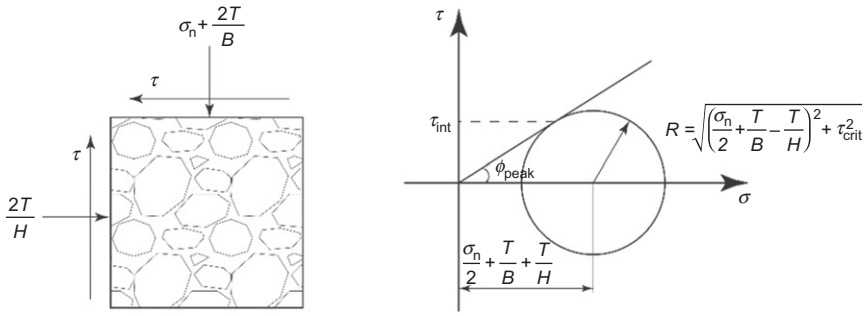

Figure 14. Stress analysis of the element inside the soilbags

expressed as

$$\tau_{crit} = \frac{1}{2}\sqrt{(\sigma_z + \sigma_x)^2 \sin^2\phi - (\sigma_z - \sigma_x)^2} \quad (6)$$

If the interfacial shear strength, τ_f, between soilbags was smaller than that of the materials filling them, τ_{crit}, only sliding along the interface occurred. Otherwise, failure of materials filling the soilbags due to deformation occurred first, followed by sliding along the interface.

To calculate the value of τ_{crit} of soilbags filled with sand and pebbles, the mobilised tensile forces T of bags under different normal stresses were determined. Separate tests were conducted by loading three soilbags stacked vertically to obtain the relationship between the tensile strain acting with the bags and the applied normal stress. Before the compression load was applied, four points were marked on the front, back, right and left sides of the surface of the soilbags in the middle layer, of which two points were marked on the warp strip and two on the weft strip. The initial distance between the points was 10 cm. A string was attached to the surface to simulate the distance between points, and a ruler with an accuracy of 0.1 mm was used to measure the length of the string. The average value of eight measurements was used to calculate the tensile force, as shown in Figure 15. Tensile force T corresponding to each value of tensile strain was then obtained from a simple tension test. A device called a 'multi-functional biaxial tensile testing machine' (Wu *et al.* 2014) was used to test a woven sheet of size 5 cm × 10 cm. The rate of extension of the sheet was 0.25 mm/min, and the results are as shown in Figure 16.

Figure 17 shows all the experimental values of τ_f (T1S and T1P) and the calculated τ_{crit} (Equation (6)) of soilbags filled with sand and pebbles. It is clear that the calculated critical shear stress of the soilbag filled with pebbles $\tau_{crit\text{-}pebble\ (calculated)}$ using Equation (6) agreed with the measured intermediate shear stress $\tau_{int\text{-}pebble\ (T1P)}$ in the T1P. This means that the intermediate shear stress causing the shear deformation of the stacked soilbags filled with pebbles can be measured by the shear test on them.

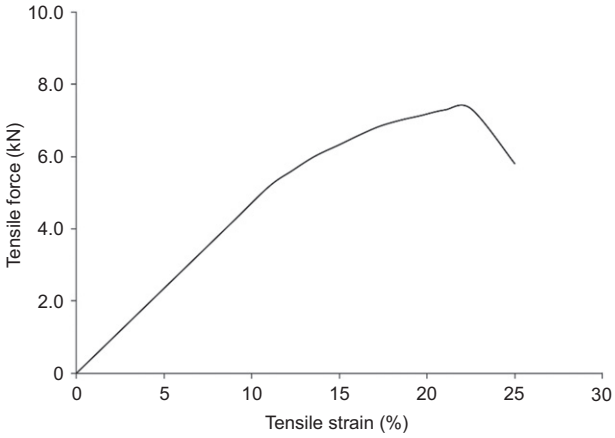

Figure 16. Tensile behaviour of the woven bags

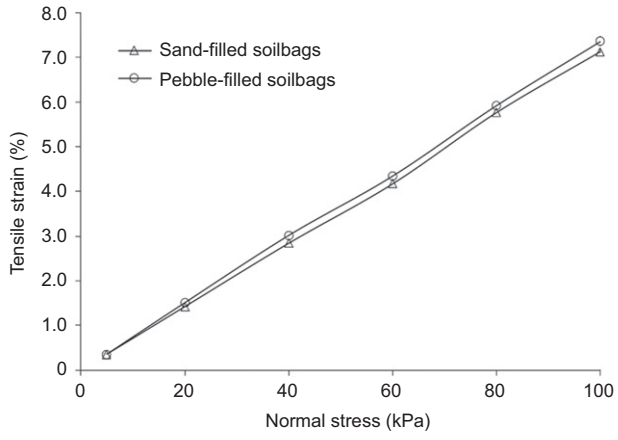

Figure 15. Tensile strain of woven bag versus normal stress applied on soilbag

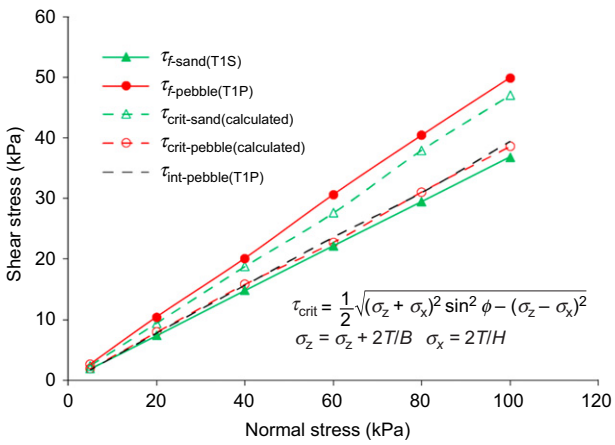

Figure 17. τ_f and τ_{crit} versus normal stress of soilbags

Figure 17 also shows that for sand-filled soilbags, $\tau_{\text{f-sand(T1S)}} < \tau_{\text{crit-sand (calculated)}}$, which means that they did not deform before sliding. On the contrary, for soilbags filled with pebbles, $\tau_{\text{f-pebble(T1P)}} > \tau_{\text{crit-pebble(calculated)}} \approx \tau_{\text{int-pebble(T1P)}}$, which means that they deformed before sliding. Note that in practice, for retaining structures built or reinforced using soilbags with strict requirements for displacement, the intermediate shear stress should be regarded as the shear strength rather than the final stress. Otherwise, the final shear stress can be used for design.

6. CONCLUSION

A series of shear tests were conducted in this study to examine the effects of materials filling the bags and interlayer arrangements on the shear strength and deformation of the stacked soilbags. Based on the results, the following conclusions can be obtained.

(1) The shear strength of soilbags with different arrangements was found to be related to the shape of the shear failure surface. This surface is the interface between soilbags when they are stacked vertically but is ladder-like when soilbags are stacked in a staggered manner.
(2) Two shear failure modes of the stacked soilbags filled with two different materials were observed. When the final shear strength of the interface was smaller than the critical shear strength of the materials filling the bags, only interlayer sliding failure occurred. Otherwise, the failure due to deformation of the materials occurred first, followed by sliding failure.

ACKNOWLEDGEMENTS

This work was supported by the National Key R&D Program of China (Grant No. 2017YFE0128900). It was also part of a project funded by the China Scholarship Council (No. 201806710071).

NOTATION

Basic SI units are given in parentheses.

B width of the soilbag (m)
F horizontal force on five layers of soilbags stacked in a staggered manner (N)
F_{T1S} shear force of soilbags without insertion (N)
F_{T2S} shear force of soilbags with insertion (N)
f_1, f_2 frictions between two layers of soilbags (N)
D_{30} fraction of soil mass that is 30% finer than
D_{50} fraction of soil mass that is 50% finer than
D_{60} fraction of soil mass that is 60% finer than
D_{90} fraction of soil mass that is 90% finer than
H height of the soilbag (m)
h height of three vertical stacked soilbags (m)
N_1, N_2 reactions at the bottom of the soilbags (N)
R radius of the Mohr circle (m)
T tensile force along the bag (N)
β ratio of F_{T2S} to F_{T1S} (dimensionless)
γ rotational shear strain (dimensionless)
ΔX rotational shear displacement (m)
θ angle of inclination of the inclined surfaces between soilbags (degrees)
μ coefficient of interface friction between soilbags (dimensionless)
$\rho_{\min}$ minimum density (Kg/m^3)
$\rho_{\max}$ minimum density (Kg/m^3)
σ normal stress produced by weight of soilbags together with stress σ_{n} (Pa)
σ_{n} applied normal stress on soilbags (Pa)
σ_x lateral stress acting on the element of the soil in the bag (Pa)
σ_z normal stress acting on the element of the soil in the bag (Pa)
τ, τ_{f} shear stress and shear stress at failure (Pa)
τ_{bag} shear stress of bags at failure (Pa)
τ_{crit} shear stress causing soilbag to deform (Pa)
$\tau_{\text{crit-pebble(calculated)}}$, $\tau_{\text{crit-sand(calculated)}}$ calculated critical shear stress of the stacked soilbags filled with pebbles and that filled with sand (Pa)
$\tau_{\text{f-sand(T1S)}}$ shear stress at failure of the stacked soilbags filled with sand in shear test T1S (Pa)
τ_{int} intermediate shear stress of stacked soilbags (Pa)
$\tau_{\text{int-pebble(T1P)}}$ intermediate shear stress of stacked soilbags filled with pebbles in shear test T1P (Pa)
τ_{pebble} shear stress of pebbles at failure (Pa)
ϕ peak friction angle (degrees)
ϕ_{bag} friction angle of woven bags (degrees)

REFERENCES

Ansari, Y., Merifield, R., Yamamoto, H. & Sheng, D. (2011). Numerical analysis of soilbags under compression and cyclic shear. *Geotextiles and Geomembranes*, **38**, No. 5, 659–668.

Basudhar, P. (2010). Modeling of soil–woven geotextile interface behavior from direct shear test results. *Geotextiles and Geomembranes*, **28**, No. 4, 403–408.

Cheng, H., Yamamoto, H. & Thoeni, K. (2016). Numerical study on stress states and fabric anisotropies in soilbags using the DEM. *Computers and Geotechnics*, **76**, 170–183.

Ding, G., Wu, J., Wang, J. & Hu, X. (2017). Effect of sand bags on vibration reduction in road subgrade. *Soil Dynamics and Earthquake Engineering*, **100**, 529–537.

Fan, K., Liu, S. H., Cheng, Y. P. & Wang, Y. S. (2019). Sliding stability analysis of a retaining wall constructed by soilbags. *Geotechnique Letters*, **9**, No. 3, 211–217.

Krahn, T., Blatz, J., Alfaro, M. & Bathurst, R. (2007). Large-scale interface shear testing of sandbag dyke materials. *Geosynthetics International*, **14**, No. 2, 119–126.

Li, Z., Liu, S. H., Wang, L. & Zhang, C. (2013). Experimental study on the effect of frost heave prevention using soilbags. *Cold Regions Science and Technology*, **85**, 109–116.

Liu, S. H. (2017). *Principle and Application of Soilbags*, Science Press, Nanjing, China.

Liu, S. H., Bai, F., Wang, Y., Wang, S. & Li, Z. (2012). Treatment for expansive soil channel slope with soilbags. *Journal of Aerospace Engineering*, **26**, No. 4, 657–666.

Liu, S. H., Gao, J. J., Wang, Y. Q. & Weng, L. P. (2014). Experimental study on vibration reduction by using soilbags. *Geotextiles and Geomembranes*, **42**, No. 1, 52–62.

Liu, S. H., Lu, Y., Weng, L. & Bai, F. (2015). Field study of treatment for expansive soil/rock channel slope with soilbags. *Geotextiles and Geomembranes*, **43**, No. 4, 283–292.

Liu, S. H., Fan, K., Chen, X., Jia, F., Mao, H. & Lin, Y. (2016). Experimental studies on interface friction characteristics of soilbags. *Chinese Journal of Geotechnical Engineering*, **38**, No. 10, 1874–1880.

Liu, S. H., Fan, K. & Xu, S. (2019). Field study of a retaining wall constructed with clay-filled soilbags. *Geotextiles and Geomembranes*, **47**, No. 1, 87–94.

Lohani, T., Matsushima, K., Aqil, U., Mohri, Y. & Tatsuoka, F. (2006). Evaluating the strength and deformation characteristics of a soil bag pile from full-scale laboratory tests. *Geosynthetics International*, **13**, No. 6, 246–264.

Matsuoka, H. & Liu, S. H. (2003). New earth reinforcement method by soilbags ('Donow'). *Soils and Foundations*, **43**, No. 6, 173–188.

Matsuoka, H. & Liu, S. H. (2014). *A new Earth Reinforcement Method Using Soilbags*, CRC Press, London, UK.

Matsushima, K., Aqil, U., Mohri, Y. & Tatsuoka, F. J. G. I. (2008). Shear strength and deformation characteristics of geosynthetic soil bags stacked horizontal and inclined. *Geosynthetics International*, **15**, No. 2, 119–135.

Portelinha, F., Zornberg, J. & Pimentel, V. (2014). Field performance of retaining walls reinforced with woven and nonwoven geotextiles. *Geosynthetics International*, **21**, No. 4, 270–284.

Wang, L. J., Liu, S. H. & Zhou, B. (2015). Experimental study on the inclusion of soilbags in retaining walls constructed in expansive soils. *Geotextiles and Geomembranes*, **43**, No. 1, 89–96.

Wang, Y. Q., Liu, K., Li, X., Ren, Q. B., Li, L. L., Zhang, Z. H. & Li, M. C. (2019). Experimental and upper-bound study of the influence of soilbag tail length on the reinforcement effect in soil slopes. *Geotextiles and Geomembranes*, **47**, No. 5, 610–617.

Wu, H., Su, Y., Cao, M. & Jiang, X. (2014). Development and application of multi-functional biaxial tensile testing machine for geosynthetics. *Chinese Journal of Geotechnical Engineering*, **36**, No. 1, 170–175.

Xu, Y., Huang, J., Du, Y. & Sun, D. A. (2008). Earth reinforcement using soilbags. *Geotextiles and Geomembranes*, **26**, No. 3, 279–289.

The Editor welcomes discussion on all papers published in Geosynthetics International. Please email your contribution to discussion@geosynthetics-international.com